Cancer Immunology, Immunotherapy (2021) 70:137–151
https://doi.org/10.1007/s00262-020-02668-8

ORIGINAL ARTICLE

ZFHX3 mutation as a protective biomarker for immune checkpoint blockade in non-small cell lung cancer

Jiexia Zhang[1] · Ningning Zhou[2] · Anqi Lin[3] · Peng Luo[3] · Xin Chen[4] · Huojin Deng[4] · Shijun Kang[5] · Linlang Guo[6] · Weiliang Zhu[3] · Jian Zhang[3]

Received: 22 March 2020 / Accepted: 8 July 2020 / Published online: 11 July 2020

Abstract

To date, immunotherapy has opened a new chapter in the treatment of lung cancer. Precise biomarkers can help to screen subpopulations of lung cancer to provide the best treatment. Multiple studies suggest that specific gene mutations may be predictive markers in guiding non-small cell lung cancer (NSCLC) immune checkpoint inhibitor (ICI) treatment. A published immunotherapy cohort with mutational and survival data for 350 NSCLC patients was used. First, the mutational data of the immunotherapy cohort were used to identify gene mutations related to the prognosis of ICI therapy. The immunotherapy cohort and TCGA-NSCLC cohort were further studied to elucidate the relationships between specific gene mutations and tumor immunogenicity, antitumor immune response capabilities, and immune cell and mutation counts in the DNA damage response (DDR) pathway. In the immunotherapy cohort ($N=350$), ZFHX3 mutations were an independent predictive biomarker for NSCLC patients receiving ICI treatment. Significant differences were observed between ZFHX3-mutant (ZFHX3-MT) and ZFHX3-wild type (ZFHX3-WT) patients regarding the overall survival (OS) time ($P<0.001$, HR = 0.26, 95% CI 0.17–0.41). ZFHX3-MT is significantly associated with higher tumor mutation burden (TMB) and neoantigen load (NAL), and ZFHX3-MT positively correlates with known immunotherapy response biomarkers, including T-cell infiltration, immune-related gene expression, and mutation counts in the DDR pathway in NSCLC. ZFHX3-MT is closely related to longer OS in NSCLC patients treated with ICIs, suggesting that ZFHX3 mutations be used as a novel predictive marker in guiding NSCLC ICI treatment.

Keywords Non-small cell lung cancer · ZFHX3 · Immune checkpoint inhibitor · Biomarker

Abbreviations

CTLA-4	Cytotoxic T lymphocyte antigen 4
GEP	Gene expression profile
Mb	Megabase
NSCLC	Non-small-cell lung cancer

Jiexia Zhang, Ningning Zhou, Anqi Lin, Peng Luo, and Xin Chen have contributed equally to this work.

Electronic supplementary material The online version of this article (https://doi.org/10.1007/s00262-020-02668-8) contains supplementary material, which is available to authorized users.

✉ Linlang Guo
linlangg@yahoo.com

✉ Weiliang Zhu
duarion@126.com

✉ Jian Zhang
blacktiger@139.com

[1] National Clinical Research Center for Respiratory Disease, State Key Laboratory of Respiratory Disease, Department of Medicine, Guangzhou Institute of Respiratory Disease, 151 Yanjiang Road, Guangzhou 510120, Guangdong Province, People's Republic of China

[2] Department of Medical Oncology, State Key Laboratory of Oncology in South China, Collaborative Innovation Center for Cancer Medicine, Sun Yat-Sen University Cancer Center, Guangzhou, China

[3] Department of Oncology, Zhujiang Hospital, Southern Medical University, 253 Gongye Road, Guangzhou 510282, People's Republic of China

[4] Department of Pulmonary and Critical Care Medicine, Zhujiang Hospital, Southern Medical University, 253 Gongye Road, Guangzhou 510282, People's Republic of China

[5] Department of Oncology, Nanfang Hospital, Southern Medical University, Guangzhou, China

[6] Department of Pathology, Zhujiang Hospital, Southern Medical University, 253 Gongye Road, Guangzhou 510282, People's Republic of China

ORR	Objective response rate
OS	Overall survival
PD	Progression of disease
PD-(L)1	Programmed cell death (ligand) 1
PFS	Progression-free survival
ICIs	Immune checkpoint inhibitors
TCGA	The cancer genome atlas
GSEA	Gene set enrichment
TMB	Tumor mutational burden
ZFHX3-MT	ZFHX3-mutant
ZFHX3-WT	ZFHX3-wildtype
MSK-IMPACT	The Memorial Sloan Kettering-Integrated Mutation Profiling of Actionable Cancer Targets
NAL	Neoantigen loads
LUAD	Lung adenocarcinoma
LUSC	Lung squamous cell carcinoma
DDR	DNA damage response
GDSC	The genomics of drug sensitivity in cancer
WES	Whole-exome sequencing
CTL	Cytotoxic T lymphocyte
FA	Fanconi anemia
NHEJ	Non-homologous end joining
BER	Base excision repair
MMR	Mismatch repair
NER	Nucleotide excision repair
DSB	Double-strand breaks
SSB	Single-strand breaks
HR	Homologous recombination

Introduction

Lung cancer ranks first in the incidence and mortality of malignant tumors worldwide. Non-small cell lung cancer (NSCLC) accounts for approximately 80–85% of lung cancer, and more than 50% of patients have distant metastasis at the time of diagnosis. The 5-year survival rate in patients with NSCLC is less than 15–20% [1]. In recent years, with the discovery of immune checkpoint molecules, including programmed cell death protein-1 (PD-1), its ligand PD-L1, and cytotoxic T-lymphocyte-associated protein 4 (CTLA-4), immunotherapy has become one of the most promising treatment strategies for lung cancer. In advanced NSCLC, the response rate of treatment with immune checkpoint inhibitor (ICIs) is approximately 17–21%, and some patients have a very long-lasting response [2]. However, many patients do not benefit from ICIs, and immunotherapy lacks precise biomarkers to predict efficacy [3, 4]. Therefore, identifying biomarkers to screen dominant populations for ICI efficacy is particularly important.

In recent years, studies have shown that PD-L1 expression, tumor mutation burden (TMB), microsatellite instability, mismatch repair gene deficiency, special gene mutations, tumor immune microenvironment, gene expression profiles (GEPs), and antigen presentation defects may serve as predictive markers for the efficacy of ICIs [5]. However, these markers also have certain limitations, so precise predictive markers for ICI treatment still need to be explored [6, 7].

Studies have shown a correlation between specific gene mutations and the sensitivity of ICIs [8–10]. The loss of TP53 function is associated with increased PD-L1 expression and increased TMB [11–13]. In NSCLC, EGFR mutations may cause the upregulation of PD-L1 expression [14]. In multiple cancers, TET1 mutations were strongly associated with longer progression-free survival (PFS) and improved overall survival (OS) in patients receiving ICI treatment [10]. In addition, mutations in the DNA damage response and repair (DDR) pathway can increase tumor immunogenicity by accumulating incorrect DNA damage responses to increase the efficacy of ICI treatment [15, 16]. The above results suggest that gene mutations may be a novel predictive biomarker for ICIs in NSCLC.

In this study, we used an NSCLC immunotherapy cohort (reported by Samstein et al. [17]) with mutational and clinical data to further evaluate the association between specific gene mutations and the efficacy of ICIs in NSCLC. The results suggest that ZFHX3 mutations can be used as an independent predictive biomarker for NSCLC patients receiving ICIs. In addition, ZFHX3 mutations are strongly associated with improved OS, enhanced tumor immunogenicity, activated antitumor immunity, T-cell infiltration, immune-related gene expression, and mutation counts in the DDR pathway.

Materials and methods

Clinical samples and cancer cell lines

To assess the relationship between gene mutations and ICI efficacy in NSCLC patients, we collected an anti-PD-(L)1 monotherapy or in combination with anti-CTLA-4 NSCLC clinical cohort ($N = 350$). The R package "TCGAbiolinks" [18] was used to download The Cancer Genome Atlas (TCGA)-Lung Adenocarcinoma (LUAD) and TCGA-Lung Squamous Cell Carcinoma (LUSC) cohorts, including mRNA expression profiling data, somatic mutation data and patient prognosis information from TCGA. Then, the TCGA-LUAD and TCGA-LUSC cohorts were combined into the TCGA-NSCLC cohort for subsequent analysis. The unit of gene expression was pan-cancer normalized log2 (fragments per kilobase of exon model per million mapped fragments [FPKM] + 1). In addition, we used cBioPortal

(https://www.cbioportal.org) to download the survival data (disease-free survival, DFS) of the TCGA-LUAD and TCGA-LUSC patients [19]. We downloaded data for 67 NSCLC cell lines with whole-exome sequencing (WES) and drug sensitivity data from the Genomics of Drug Sensitivity in Cancer (GDSC) database. We downloaded an independent cohort including 75 patients with NSCLC treated with nivolumab plus ipilimumab as part of the CheckMate-012 study [20].

Identification of survival-related gene mutations and establishment of prognostic gene mutations

The mutational data of the immunotherapy cohort were used to identify specific mutated genes related to the prognosis of ICIs. Univariate and multivariate Cox regression model analyses and Kaplan–Meier analysis were used to evaluate the predictive function of specific mutated genes in ICI treatment. The detailed analysis process is shown in Supplementary Fig. S1.

Correlation analysis of tumor immunogenicity and immune characteristics

We used the CIBERSORT web portal (https://cibersort.stanford.edu/) to evaluate the 22 immune cell infiltration status of the TCGA-NSCLC cohort [21]. The immune-associated gene list, neoantigen load (NAL) data, immune-related genes, and their functional classifications were from Thorsson et al. [22], and the expression levels of these genes were quantified as log2 (FPKM + 1). We took the somatic called variants in the TCGA-NSCLC cohort as the raw mutation count. In addition, we used 38 Mb as the estimate of the exome size [23].

Pathway enrichment analysis and gene sets related to the DDR pathway

For gene annotation enrichment analysis, the clusterProfiler R package was used, and $P < 0.05$ indicated a significant difference for Gene Ontology (GO) terms, Kyoto Encyclopedia of Genes and Genomes (KEGG) pathways and Reactome pathways [24]. The gene set enrichment analysis (GSEA) gene set and the DDR pathway gene set were obtained from the Broad Institute Molecular Signatures Database (MSigDB) [25]. The details of DDR-related gene sets are shown in Supplementary Table. S1.

Statistical analysis

The association between ZFHX3 status and TMB, NAL, immune gene expression, and immune cells was examined using the Mann–Whitney *U* test. Assessment of the association between the top 20 mutated genes' rate and ZFHX3 status was performed with Fisher's exact test and the Chi-square test. The DFS and OS probabilities of ZFHX3-mutant (ZFHX3-MT) and ZFHX3-wild type (ZFHX3-WT) patients were analyzed by the Kaplan–Meier method, the log-rank test, and univariate and multivariate Cox proportional hazard regression analyses. $P < 0.05$ was considered statistically significant, and all statistical tests were two-sided. R software (version 3.6) was used for statistical analysis. The R package ComplexHeatmap was employed to visualize the mutational landscape and create a heatmap [26].

Results

ZFHX3 gene mutation is an independent predictive biomarker for the treatment response of NSCLC patients receiving ICIs

We used cBioPortal to collect a published cohort study of NSCLC immunotherapy patients (Samstein et al.), including 350 patients receiving ICIs (anti-PD-(L)1 monotherapy or in combination with anti-CTLA-4) with available mutational and clinical data to further explore the relationship between gene mutations and the prognosis of ICIs (Supplementary Fig. S1). Gene mutations (mutation frequency > 5% cases) were analyzed by a univariate Cox regression model. The analysis showed that the mutation counts, the types of immunotherapy drugs, and specific gene mutations (PBRM1, ZFHX3, NTRK3, EPHA5, EPHA7, EPHA3, MGA, and PTPRD) were related to the prognosis of immunotherapy, and the differences were significant (Fig. 1a, $P < 0.05$). Among them, low mutation counts, PBRM1 mutations, and immune monotherapy were associated with a worse prognosis of immunotherapy; on the contrary, other gene mutations, including ZFHX3, NTRK3, EPHA5, EPHA7, EPHA3, and MGA, were associated with a better prognosis of immunotherapy (Fig. 1b). Statistically significant ($P < 0.05$) indicators in univariate Cox analysis were introduced into the multivariate Cox regression model, and the results showed that ZFHX3 mutations were associated with a better prognosis for immunotherapy and that PBRM1 mutations were associated with a worse prognosis for immunotherapy (Fig. 1c; Supplementary Fig. 2a). Survival analysis showed that the OS of patients with ZFHX3-MT NSCLC was significantly longer than that of patients with ZFHX3-WT ($P < 0.001$, HR = 0.26, 95% CI 0.17 – 0.41; Fig. 1d). In addition, subgroup analysis showed that patients with ZFHX3-MT LUAD had a longer OS after ICI treatment than patients with ZFHX3-WT (Fig. 1g, $P = 0.004$, HR = 0.3, 95% CI 0.18–0.51). To further validate the predictive function of ZFHX3-MT and TMB on OS benefit, Kaplan–Meier

A

Univariable cox	Type	No.of Patients	No.of Events	HR	HR (95CI%)	P-value
TMB Status	Low-Mutation	258	176		Reference	
	High-Mutation	92	43		0.55 (0.39, 0.77)	<0.001
Drug Type	Combination	21	9		Reference	
	Monotherapy	329	210		2.47 (1.26, 4.86)	0.009
PBRM1 Status	WT	332	204		Reference	
	MT	18	15		2.10 (1.24, 3.56)	0.006
ZFHX3 Status	WT	323	213		Reference	
	MT	27	6		0.26 (0.11, 0.58)	0.001
NTRK3 Status	WT	330	213		Reference	
	MT	20	6		0.36 (0.16, 0.81)	0.013
EPHA5 Status	WT	321	208		Reference	
	MT	29	11		0.47 (0.26, 0.87)	0.016
EPHA7 Status	WT	332	214		Reference	
	MT	18	5		0.34 (0.14, 0.82)	0.016
EPHA3 Status	WT	313	202		Reference	
	MT	37	17		0.58 (0.35, 0.95)	0.031
MGA Status	WT	330	211		Reference	
	MT	20	8		0.46 (0.23, 0.94)	0.033
PTPRD Status	WT	307	198		Reference	
	MT	43	21		0.62 (0.40, 0.98)	0.040

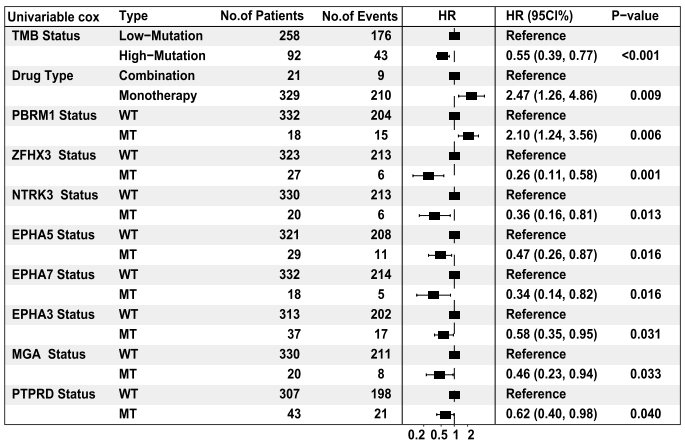

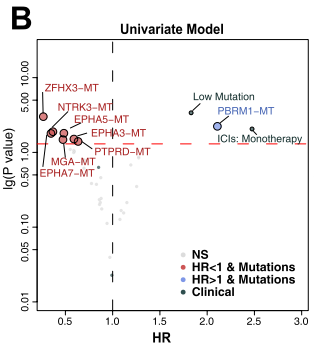

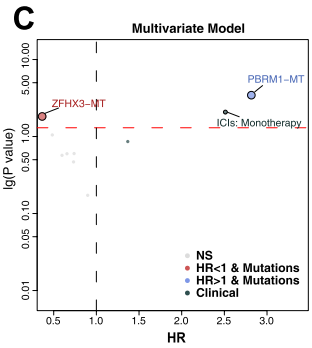

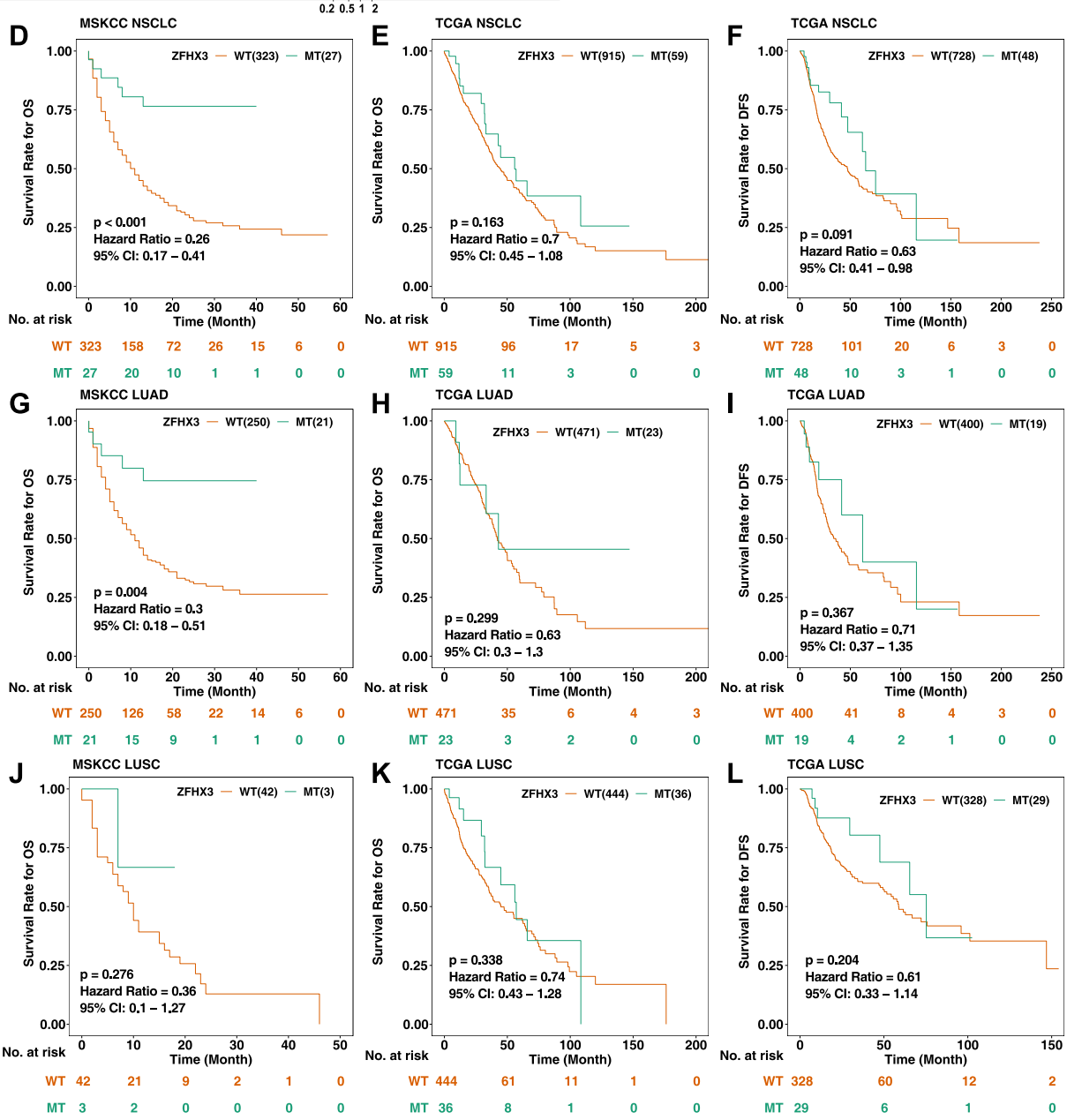

◂**Fig. 1** Results of Cox proportional hazard regression analysis for the ICI-treated NSCLC cohort (Samstein et al. $N=350$) and survival curves for patients with NSCLC stratified by ZFHX3 status. **a** Forest plots showing the loge hazard ratio (95% confidence interval). Cox p values less than 0.05 are shown. Bubble plot showing the result of univariate **b** and multivariate **c** Cox proportional hazard regression analysis between ZFHX3-MT and ZFHX3-WT tumors. **d** Kaplan–Meier estimates of OS in the ICI-treated NSCLC cohort comparing patients with ZFHX3-MT with their respective counterparts without ZFHX3-MT. Patients (NSCLC) who harbored ZFHX3 mutations showed a better prognosis for ICI-based immunotherapy ($P<0.001$, log-rank test). **e** Kaplan–Meier estimates of OS in the TCGA-NSCLC cohort comparing patients with ZFHX3-MT with their respective counterparts without ZFHX3-MT. **f** Kaplan–Meier estimates of DFS in the TCGA-NSCLC cohort comparing patients with ZFHX3-MT with their respective counterparts without ZFHX3-MT.**g** Kaplan–Meier estimates of OS in the ICI-treated LUAD cohort comparing patients with ZFHX3-MT with their respective counterparts without ZFHX3-MT. Patients (LUAD) who harbored ZFHX3 mutations showed a better prognosis for ICI-based immunotherapy. **h** Kaplan–Meier estimates of OS comparing patients in the TCGA-LUAD cohort with ZFHX3-MT with their respective counterparts without ZFHX3-MT. **i** Kaplan–Meier estimates of DFS in the TCGA-LUAD cohort comparing patients with ZFHX3-MT with their respective counterparts without ZFHX3-MT. **j** Kaplan–Meier estimates of OS in the ICI-treated LUSC cohort comparing patients with ZFHX3-MT with their respective counterparts without ZFHX3-MT. **k** Kaplan–Meier estimates of OS in the TCGA-LUSC cohort comparing patients with ZFHX3-MT with their respective counterparts without ZFHX3-MT. **l** Kaplan–Meier estimates of DFS in the TCGA-LUSC cohort comparing patients with ZFHX3-MT with their respective counterparts without ZFHX3-MT

curves were used to investigating the prognostic impact of ZFHX3 status and TMB status in the ICI-treated cohort from Samstein et al. ($N=350$). In patients with known TMB status (according to a median of TMB; $N=350$); 92 of them were TMB-High, while 27 were ZFHX3-MT, and 18 patients were both TMB-high and ZFHX3-MT. Notably, in patients with TMB-Low, ZFHX3-MT could equal to that of TMB-High patients (Group 3 vs Group 2: $p=0.6027$; Supplementary Fig. 2b). As expected, the longest OS of patients with ZFHX3-MT and TMB-High was observed (Supplementary Fig. 2c, Group 3 vs Group 1: $p=4e\text{-}04$; Group 3 vs Group 2: $p=0.0046$; Group 3 vs Group 4: $p=0.0327$). The OS benefit from ICI treatment was worst in the ZFHX3-WT and TMB-Low compared with other groups. (Supplementary Fig. 2c). In a validation cohort ($N=75$; reported by Hellmann et. al [20]), the PFS benefit from ICI treatment was more prominent in the ZFHX3-MT group than that in the ZFHX3-WT group (Supplementary Fig. 2d, median PFS, not reached in the ZFHX3-MT group versus 7.8 months in the ZFHX3-WT group). However, there was no numerically significant PFS benefit ($p=0.08$, HR = 0.21 [95%Cl, 0.08 to 0.64]), probably due to the limited sample size of the ZFHX3-MT group ($N=4$). Therefore, ZFHX3 mutations can be used as an independent predictive biomarker for NSCLC patients receiving ICI treatment. To confirm that the OS benefit from ICI treatment in patients with ZFHX3-MT was not simply attributed to its general prognostic impact, we further evaluated the survival differences between ZFHX3-MT and ZFHX3-WT patients in the non-ICI-treated cohort (TCGA cohort). The relationship between ZFHX3 mutations and the OS and DFS of TCGA-NSCLC/LUAD/LUSC was further explored. There was no significant difference in the prognosis of LUAD/LUSC (Fig. 1e–l).

Correlation of ZFHX3 mutations with other gene mutations and clinical characteristics

To further explore the clinical characteristics of patients with ZFHX3 mutations, we further analyzed the relationships between clinical characteristics (such as age, sex, immunotherapy drug type, smoking history, and clinical stage) and ZFHX3 mutations, and the results showed that there was no statistical difference in the correlations between these clinical characteristics and ZFHX3 mutations (Fig. 2a–b). In contrast, patients with ZFHX3 mutations had higher TMB. The types of ZFHX3 mutations in the immunotherapy and TCGA-NSCLC cohorts were mostly missense mutations (71.43% and 86.57%), nonsense mutations (14.29% and 5.97%), and frameshift mutations (10.71% and 7.46%). In contrast, there was no splice site in the ZFHX3 mutation type. The mutational landscape of the immunotherapy cohort is shown in Fig. 2a. In the immunotherapy cohort, the mutation frequency of genes in ZFHX3-MT patients was usually higher than that in ZFHX3-WT patients, such as TP53 (81% vs 67%), PTPRD (30% vs 12%), EPHA3 (26% vs 10%), and SMARCA4 (22% vs 10%) mutations. In the TCGA-NSCLC cohort (Fig. 2b), patients with ZFHX3-MT were often accompanied by other genetic mutations, including TP53 mutations (77% vs 66%), TTN mutations (75% vs 60%), and CSMD3 mutations (55% vs 41%), MUC16 mutations (55% vs 41%), etc. For detailed results, see Supplementary Table S2. Figure 2c shows the mutation sites of the ZFHX3 gene, including p.K2190, p.M2386I, p.G2893R, p.F2994L, p.Q2186L, p.T2316I, p.D2318N, p.M2881V, etc. The somatic mutation sites of the ZFHX3 gene were more evenly distributed and did not include any annotated functional hotspot mutations from 3D Hotspots (https://www.3dhotspots.org). In the TCGA database cohort of 33 tumor sample types, the statistical analysis of the frequency of ZFHX3 gene mutations (Fig. 2d) showed that the mutation rates of ZFHX3 in NSCLC, LUAD, and LUSC were 6.5% (67/1026), 5.0% (26/522), and 8.1% (41/504), respectively. Among these 33 cancer types, the average mutation rate of ZFHX3 is 5.2%, of which 27 mutation rates are higher than 1%. The gastrointestinal tract and urogenital system (including UCEC, STAD, COAD, etc.) are among the organs with the highest mutation rates.

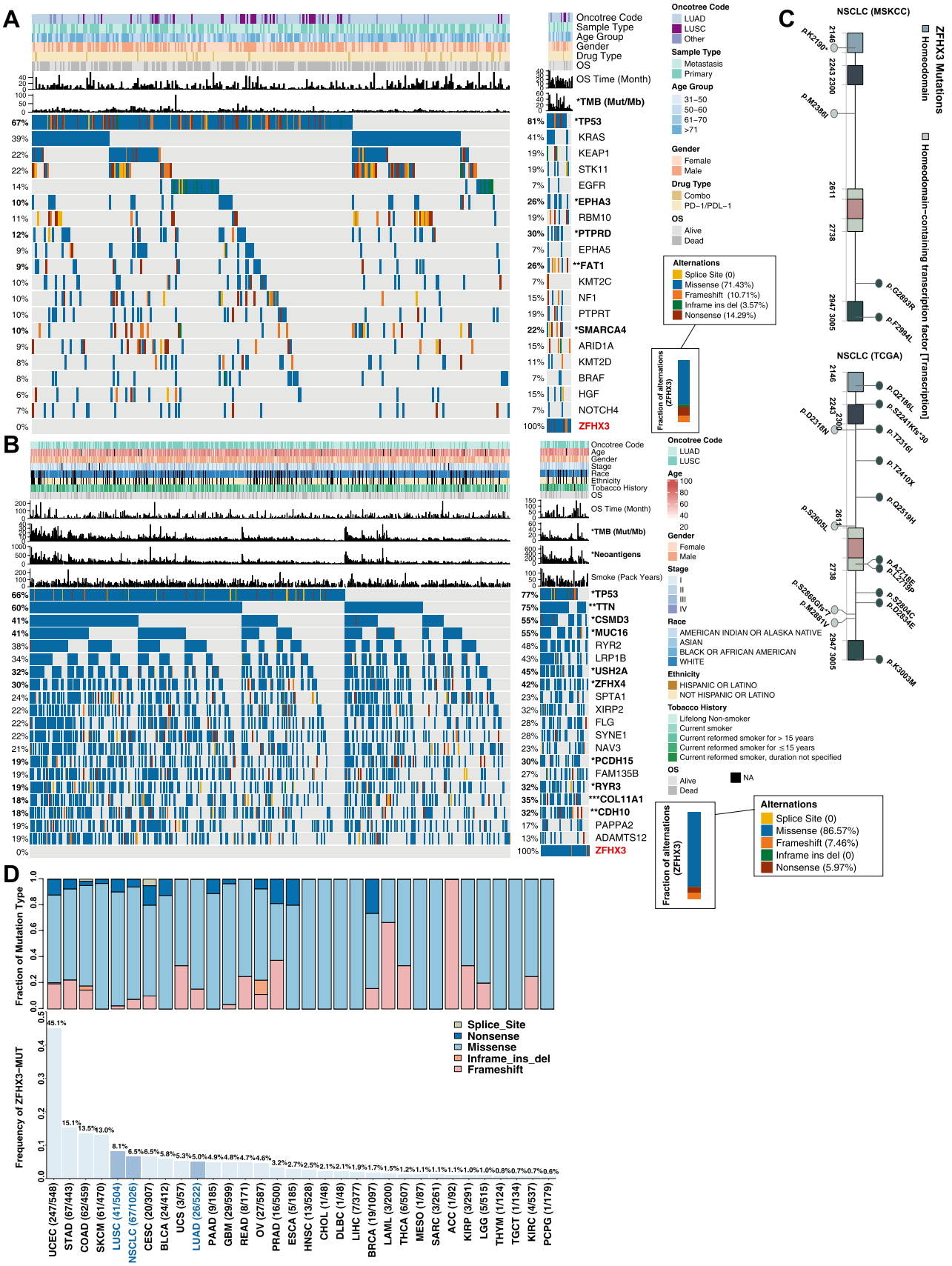
A
Oncotree Code
Sample Type
Age Group
Gender
Drug Type
OS
OS Time (Month)
*TMB (Mut/Mb)
67% *TP53
39% KRAS
22% KEAP1
22% STK11
14% EGFR
10% *EPHA3
11% RBM10
12% *PTPRD
9% EPHA5
9% **FAT1
10% KMT2C
10% NF1
10% PTPRT
10% *SMARCA4
9% ARID1A
8% KMT2D
8% BRAF
6% HGF
7% NOTCH4
0% ZFHX3
Oncotree Code
LUAD
LUSC
Other
Sample Type
Metastasis
Primary
Age Group
31–50
50–60
61–70
>71
Gender
Female
Male
Drug Type
Combo
PD–1/PDL–1
OS
Alive
Dead
Alternations
Splice Site (0)
Missense (71.43%)
Frameshift (10.71%)
Inframe ins del (3.57%)
Nonsense (14.29%)
Fraction of alternations (ZFHX3)
B
Oncotree Code
Age
Gender
Stage
Race
Ethnicity
Tobacco History
OS
OS Time (Month)
*TMB (Mut/Mb)
*Neoantigens
Smoke (Pack Years)
66% *TP53
60% **TTN
41% *CSMD3
41% *MUC16
38% RYR2
34% LRP1B
32% *USH2A
30% *ZFHX4
24% SPTA1
22% XIRP2
22% FLG
22% SYNE1
21% NAV3
19% *PCDH15
19% FAM135B
19% *RYR3
18% ***COL11A1
18% **CDH10
19% PAPPA2
19% ADAMTS12
0% ZFHX3
Oncotree Code
LUAD
LUSC
Age
Gender
Female
Male
Stage
I
II
III
IV
Race
AMERICAN INDIAN OR ALASKA NATIVE
ASIAN
BLACK OR AFRICAN AMERICAN
WHITE
Ethnicity
HISPANIC OR LATINO
NOT HISPANIC OR LATINO
Tobacco History
Lifelong Non-smoker
Current smoker
Current reformed smoker for > 15 years
Current reformed smoker for ≤15 years
Current reformed smoker, duration not specified
OS
Alive
Dead
NA
Alternations
Splice Site (0)
Missense (86.57%)
Frameshift (7.46%)
Inframe ins del (0)
Nonsense (5.97%)
Fraction of alternations (ZFHX3)
C
NSCLC (MSKCC)
ZFHX3 Mutations
Homeodomain
Homeodomain-containing transcription factor [Transcription]
p.K2190*
p.M2398I
p.G2883R
p.F2994L
NSCLC (TCGA)
p.Q2186L
p.S2241Kfs*30
p.D2318N
p.T2316I
p.T2410X
p.Q2519H
p.S2605L
p.A2719E
p.L2719P
p.S2868Gfs*7
p.M2881V
p.S2604C
p.D2634E
p.K3003M
D
Fraction of Mutation Type
Splice_Site
Nonsense
Missense
Inframe_ins_del
Frameshift
Frequency of ZFHX3−MUT
45.1%
15.1%
13.5%
3.0%
8.1%
6.5%
6.5%
5.8%
5.3%
5.0%
4.9%
4.8%
4.7%
4.6%
3.2%
2.7%
2.5%
2.1%
2.1%
1.9%
1.7%
1.5%
1.2%
1.1%
1.1%
1.1%
1.0%
1.0%
0.8%
0.7%
0.7%
0.6%
UCEC (247/548)
STAD (67/443)
COAD (62/459)
SKCM (61/470)
LUSC (41/504)
NSCLC (67/1026)
CESC (20/307)
BLCA (24/412)
UCS (3/57)
LUAD (26/522)
PAAD (9/185)
GBM (29/599)
READ (8/171)
OV (27/587)
PRAD (16/500)
ESCA (5/185)
HNSC (13/528)
CHOL (1/48)
DLBC (1/48)
LIHC (7/377)
BRCA (19/1097)
LAML (3/200)
THCA (6/507)
MESO (1/87)
SARC (3/261)
ACC (1/92)
KIRP (3/291)
LGG (5/515)
THYM (1/124)
TGCT (1/134)
KIRC (4/537)
PCPG (1/179)

◂**Fig. 2** Mutational landscape, clinical information of NSCLC patients, and the characteristics of ZFHX3 mutations in patients (NSCLC and each cancer type in TCGA). **a** Top 20 frequently mutated genes in NSCLC in the Samstein cohort (ICI-treated). The genes were ranked by the mutation frequency in NSCLC patients. The alteration type, ZFHX3 status, sex, histological subtype, OS status, OS time, treatment type, and age group are annotated. Significantly different genes are highlighted in bold (significance was calculated using Fisher's exact test). **b** Top 20 frequently mutated genes in NSCLC in the TCGA-NSCLC cohort. The genes were ranked by the mutation frequency in NSCLC patients. The alteration type, survival status, survival time, ZFHX3 status, histological subtype, clinical stage, age, race, sex, tobacco smoking history, and number of pack-years smoked are annotated. **c** Lollipop plot shows the distribution of ZFHX3 mutations in the ICI-treated cohort (left panel) and TCGA-NSCLC cohort. **d** The proportion of ZFHX3-MT tumors identified for each cancer type in TCGA. The numbers above the barplot indicate the alteration frequency, and the numbers close to the cancer names indicate the number of ZFHX3-MT patients and the total number of patients. The fractions of mutation types of ZFHX3-MT tumors identified for each cancer type in TCGA (top panel)

Associations of ZFHX3 mutations with enhanced immunogenicity and activated antitumor immunity

To investigate the immune characteristics of ZFHX3-MT NSCLC, we compared the differences in the expression patterns of immune-related genes between ZFHX3-MT and ZFHX3-WT tumors (Fig. 3a). The results showed that the expression of antigen-presentation-related molecules, stimulating immune-related ligands and receptors and cosuppressor molecules in patients with ZFHX3-MT were usually upregulated. Figure 3b shows that the expression of chemokines such as CXCL10 (FPKM: 72.8 vs 40.0) and CXCL9 (FPKM: 53.1 vs 35.9) in the ZFHX3-MT group was significantly upregulated. ZFHX3-MT tumors had a higher expression of mRNAs related to cytolytic activity, such as GZMA (FPKM: 16.0 vs 13.3), than ZFHX3-WT tumors. In addition, the ZFHX3-MT group had significantly increased immune checkpoint gene profiles, such as CD274, LAG3, PDCD1, PDCD1LG2, and TIGIT.

We compared tumor immunogenicity between ZFHX3-MT and ZFHX3-WT tumors. The TMB of ZFHX3-MT tumors in the immunotherapy cohort (Fig. 3c, $P < 0.0001$) and TCGA-NSCLC cohort (Fig. 3f, $P < 0.0001$) was significantly higher than that of ZFHX3-WT tumors. The NAL of ZFHX3-MT tumors in the TCGA-NSCLC cohort was also significantly higher (Fig. 3f, $P < 0.0001$), indicating that ZFHX3-MT is associated with increased tumor immunogenicity. Subgroup analysis showed that ZFHX3-MT in LUAD is associated with increased TMB (Fig. 3d: $P < 0.0001$; Fig. 3g: $P < 0.0001$) and NAL (Fig. 3g: $P < 0.0001$). In addition, ZFHX3-MT in TCGA-LUSC has a higher TMB ($P < 0.01$) and NAL ($P < 0.001$).

Patterns of immune cells and transcriptome traits based on MET status

To further study the tumor immune microenvironment of ZFHX3-MT NSCLC, we used the CIBERSORT algorithm to estimate the TCGA-NSCLC immune cell infiltration status and compared the differences in immune cell infiltration patterns between ZFHX3-MT and ZFHX3-WT tumors (Fig. 4). The results showed that activated CD4 memory T cells ($P < 0.05$), M1 macrophages ($P < 0.01$), and activated dendritic cells (DCs) ($P < 0.05$) were more abundant in ZFHX3-MT tumors. This finding indicates that immune-activated cells were significantly richer in the ZFHX3-MT group. Subgroup analysis showed that in TCGA-LUAD, activated CD4 memory T cells ($P < 0.05$), monocytes ($P < 0.05$), and M1 macrophages ($P < 0.05$) were significantly higher in ZFHX3-MT tumors than in ZFHX3-WT tumors.

Further analysis of the differences in potential biological mechanisms between ZFHX3-MT and ZFHX3-WT tumors (Fig. 5) and the results of GSEA (Fig. 5a–b) showed that the immune response and cell cycle-related pathways in the ZFHX3-MT group were significantly upregulated, such as B-cell activation involved in the immune response, positive regulation of interferon – gamma production, and positive regulation of natural killer cell-mediated immunity. In addition, metabolic-related pathways were significantly downregulated in the ZFHX3-MT group (Fig. 5b), such as cholesterol metabolic process and long-chain fatty acids. The differential expression profile of core genes in some pathways is shown in Fig. 5c, and genes related to immune response and cell cycle pathways were significantly upregulated in the ZFHX3-MT group. In contrast, genes related to metabolic pathways were significantly downregulated in the ZFHX3-MT group.

Correlation between ZFHX3-MT and DDR pathway mutation characteristics

In recent years, many studies have shown that genetic mutations in the DDR pathway are related to the efficacy of ICIs [15, 16, 27], so we used the DDR gene set (Supplementary Table S1) from MSigDB to compare the differences in the number of DDR pathway mutations between ZFHX3-MT and ZFHX3-WT tumors (Fig. 6). In the immunotherapy cohort, ZFHX3-MT tumors had a significantly increased number of DDR pathway mutations (including homologous recombination (HR), single-strand breaks (SSB), DSB (double-strand breaks), NER (nucleotide excision repair), NHEJ (non-homologous end joining), etc.). In the TCGA-NSCLC cohort, the number of DDR pathway mutations in ZFHX3-MT tumors was also greater. Subgroup analysis shows that

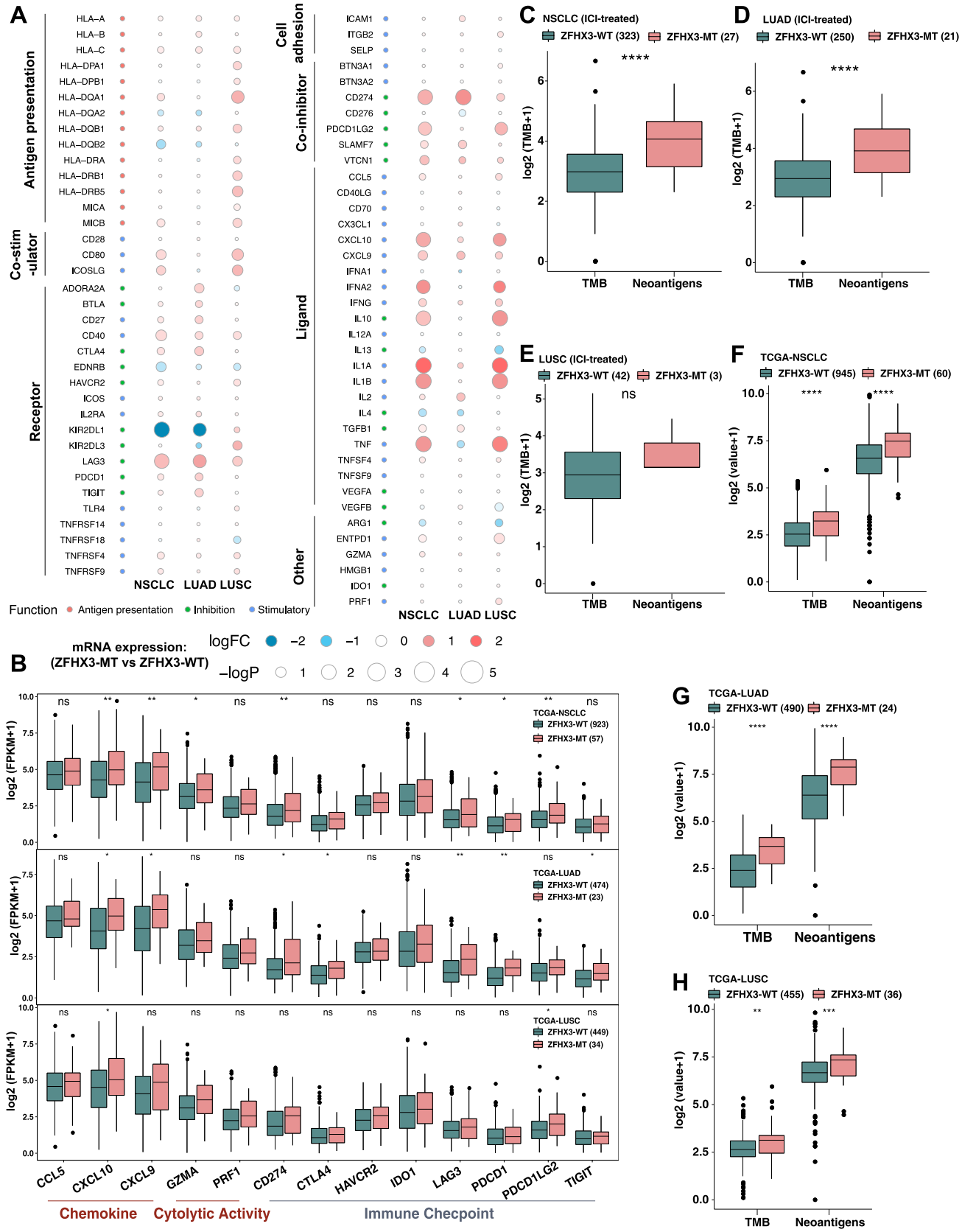
A
Antigen presentation
HLA–A
HLA–B
HLA–C
HLA–DPA1
HLA–DPB1
HLA–DQA1
HLA–DQA2
HLA–DQB1
HLA–DQB2
HLA–DRA
HLA–DRB1
HLA–DRB5
Co-stim -ulator
MICA
MICB
CD28
CD80
ICOSLG
Receptor
ADORA2A
BTLA
CD27
CD40
CTLA4
EDNRB
HAVCR2
ICOS
IL2RA
KIR2DL1
KIR2DL3
LAG3
PDCD1
TIGIT
TLR4
TNFRSF14
TNFRSF18
TNFRSF4
TNFRSF9
Cell adhesion
ICAM1
ITGB2
SELP
Co-inhibitor
BTN3A1
BTN3A2
CD274
CD276
PDCD1LG2
SLAMF7
VTCN1
Ligand
CCL5
CD40LG
CD70
CX3CL1
CXCL10
CXCL9
IFNA1
IFNA2
IFNG
IL10
IL12A
IL13
IL1A
IL1B
IL2
IL4
TGFB1
TNF
TNFSF4
TNFSF9
VEGFA
VEGFB
Other
ARG1
ENTPD1
GZMA
HMGB1
IDO1
PRF1
NSCLC LUAD LUSC
Function Antigen presentation Inhibition Stimulatory
C NSCLC (ICI-treated)
ZFHX3-WT (323) ZFHX3-MT (27)
log2 (TMB+1)
TMB Neoantigens
D LUAD (ICI-treated)
ZFHX3-WT (250) ZFHX3-MT (21)
E LUSC (ICI-treated)
ZFHX3-WT (42) ZFHX3-MT (3)
ns
F TCGA-NSCLC
ZFHX3-WT (945) ZFHX3-MT (60)
log2 (value+1)
B
mRNA expression:
(ZFHX3-MT vs ZFHX3-WT)
logFC −2 −1 0 1 2
−logP 1 2 3 4 5
log2 (FPKM+1)
TCGA-NSCLC
ZFHX3-WT (923)
ZFHX3-MT (57)
TCGA-LUAD
ZFHX3-WT (474)
ZFHX3-MT (23)
TCGA-LUSC
ZFHX3-WT (449)
ZFHX3-MT (34)
CCL5 CXCL10 CXCL9 GZMA PRF1 CD274 CTLA4 HAVCR2 IDO1 LAG3 PDCD1 PDCD1LG2 TIGIT
Chemokine Cytolytic Activity Immune Checpoint
G TCGA-LUAD
ZFHX3-WT (490) ZFHX3-MT (24)
H TCGA-LUSC
ZFHX3-WT (455) ZFHX3-MT (36)

◂**Fig. 3** ZFHX3 mutations were associated with enhanced tumor immunogenicity and activated antitumor immunity. **a** Bubble plot depicting the mean differences in immune-related gene mRNA expression between ZFHX3-MT and ZFHX3-WT tumors in the TCGA-NSCLC/LUAD/LUSC cohort. The x-axis of the bubble plot indicates different histological subtypes, and the y-axis indicates tumor-infiltrating leukocytes, immune signatures, or gene names. The size of the circle represents the difference (-log10(p-value)) of each indicated immune signature or immune-related gene between ZFHX3-MT and ZFHX3-WT tumors in each cancer type. Red indicates upregulation, while blue indicates downregulation. **b** The expression levels of immune-related genes, such as chemokines, cytolytic activity-associated genes and immune checkpoints in ZFHX3-MT tumors versus ZFHX3-WT tumors (TCGA-NSCLC, LUAD and LUSC). Comparison of TMB between ZFHX3-MT and ZFHX3-WT tumors in Samstein's NSCLC (**c**), LUAD (**d**) and LUSC (**e**) cohorts. Comparison of TMB and NAL between ZFHX3-MT and ZFHX3-WT tumors in the TCGA-NSCLC (**f**), LUAD (**g**) and LUSC (**h**) cohorts. (**b**–**h** *, $P<0.05$; **, $P<0.01$; ***, $P<0.001$, ****, $P<0.0001$, Mann–Whitney U test)

ZFHX3-MT LUAD usually also has more DDR pathway mutations. In contrast, there was no difference in the number of mutations in the DDR pathway between ZFHX3-WT and ZFHX3-MT LUSC (Supplementary Fig. S3).

Discussion

In recent years, ICIs represented by PD-1/PD-L1 inhibitors have become one of the important options for the treatment of patients with advanced NSCLC. However, ICI treatment is not effective for all patients with NSCLC, and the key to improving efficacy is to screen dominant populations. Studies have shown that specific mutated genes, such as alterations in the DDR pathway (including POLE, POLD1, MLH1, etc.) [28, 29], interferon signal pathway gene mutations [30, 31], driver gene mutations (KRAS, BRAF, ALK, EGFR, etc.) [32, 33], and other gene mutations (such as, SERPINB) [8], are related to the prognosis of ICI treatment. Therefore, we tried to explore the correlation between gene mutations and the prognosis of NSCLC immunotherapy. In this study, we systematically collected and consolidated a large amount of genomic and clinical data to evaluate the predictive function of mutations in key genes involving in NSCLC receiving ICI treatment (Supplementary Fig. S1). And we found that mutation in ZFHX3, a transcription factor that encoded four homeobox domains and 23 zinc fingers [34], was predictive of improved overall survival (OS) to

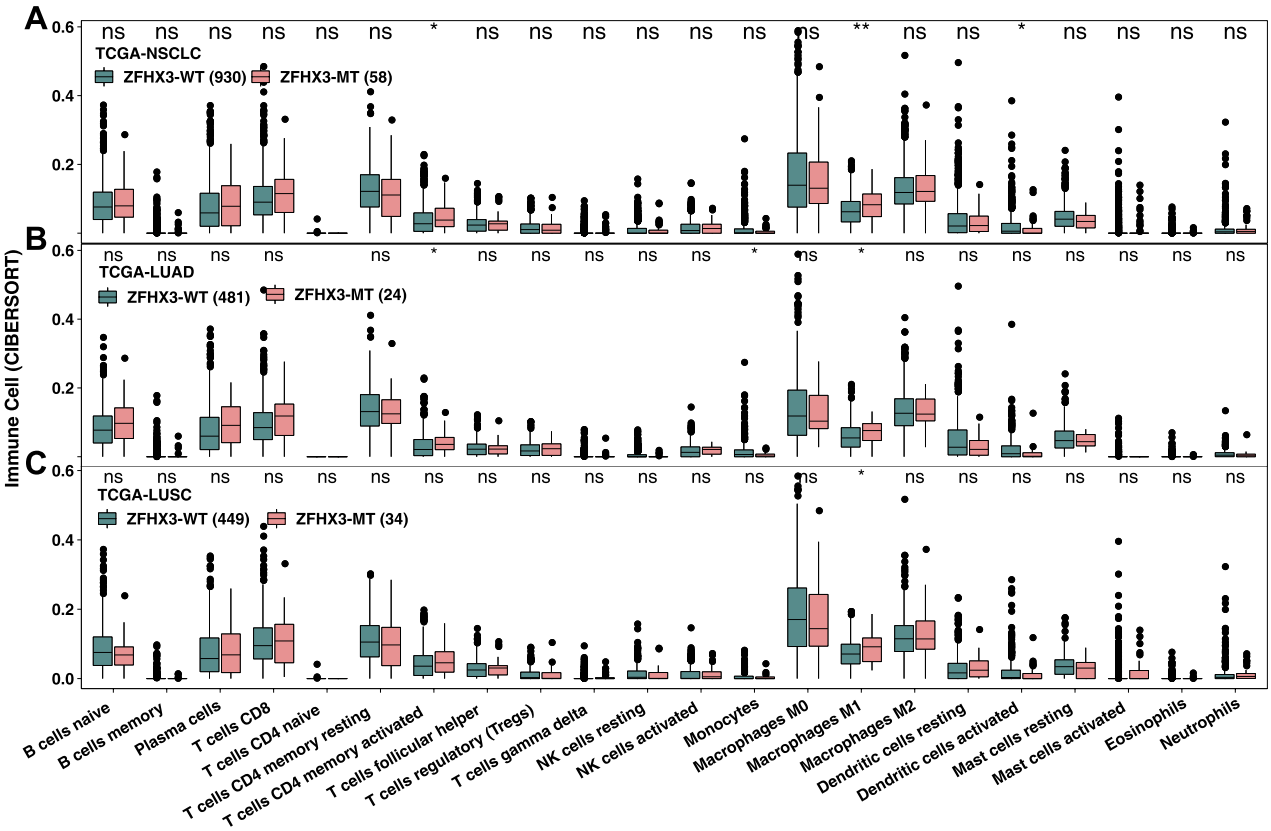

Fig. 4 Comparison of immune cells between ZFHX3-MT and ZFHX3-WT tumors in the TCGA-NSCLC (**a**), LUAD (**b**), and LUSC (**c**) cohorts. Gene expression profiles were prepared using standard annotation files, and data were uploaded to the CIBERSORT web portal (https://cibersort.stanford.edu/), with the algorithm run using the LM22 signature and 1,000 permutations

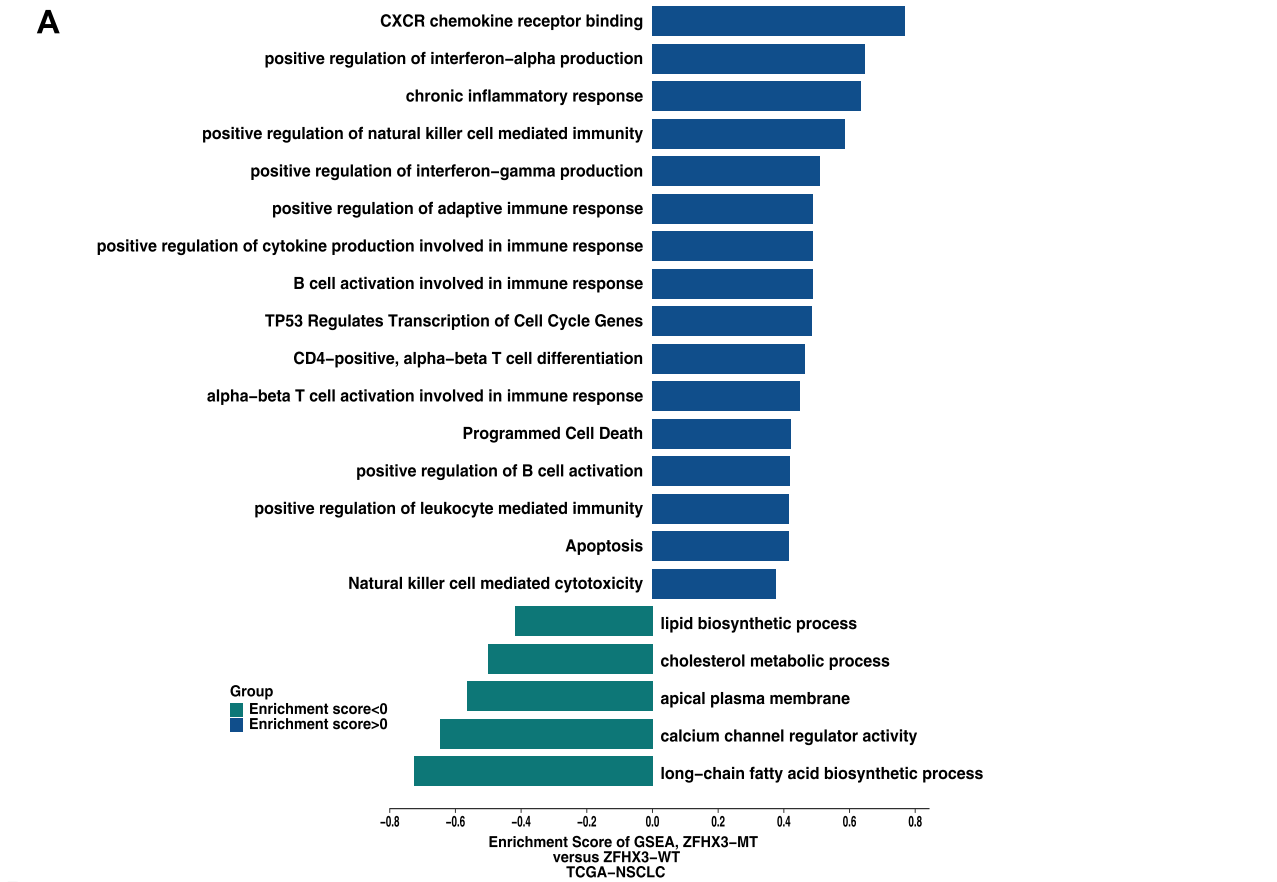
A
CXCR chemokine receptor binding
positive regulation of interferon−alpha production
chronic inflammatory response
positive regulation of natural killer cell mediated immunity
positive regulation of interferon−gamma production
positive regulation of adaptive immune response
positive regulation of cytokine production involved in immune response
B cell activation involved in immune response
TP53 Regulates Transcription of Cell Cycle Genes
CD4−positive, alpha−beta T cell differentiation
alpha−beta T cell activation involved in immune response
Programmed Cell Death
positive regulation of B cell activation
positive regulation of leukocyte mediated immunity
Apoptosis
Natural killer cell mediated cytotoxicity
lipid biosynthetic process
cholesterol metabolic process
apical plasma membrane
calcium channel regulator activity
long−chain fatty acid biosynthetic process
Group
Enrichment score<0
Enrichment score>0
−0.8 −0.6 −0.4 −0.2 0.0 0.2 0.4 0.6 0.8
Enrichment Score of GSEA, ZFHX3−MT
versus ZFHX3−WT
TCGA−NSCLC

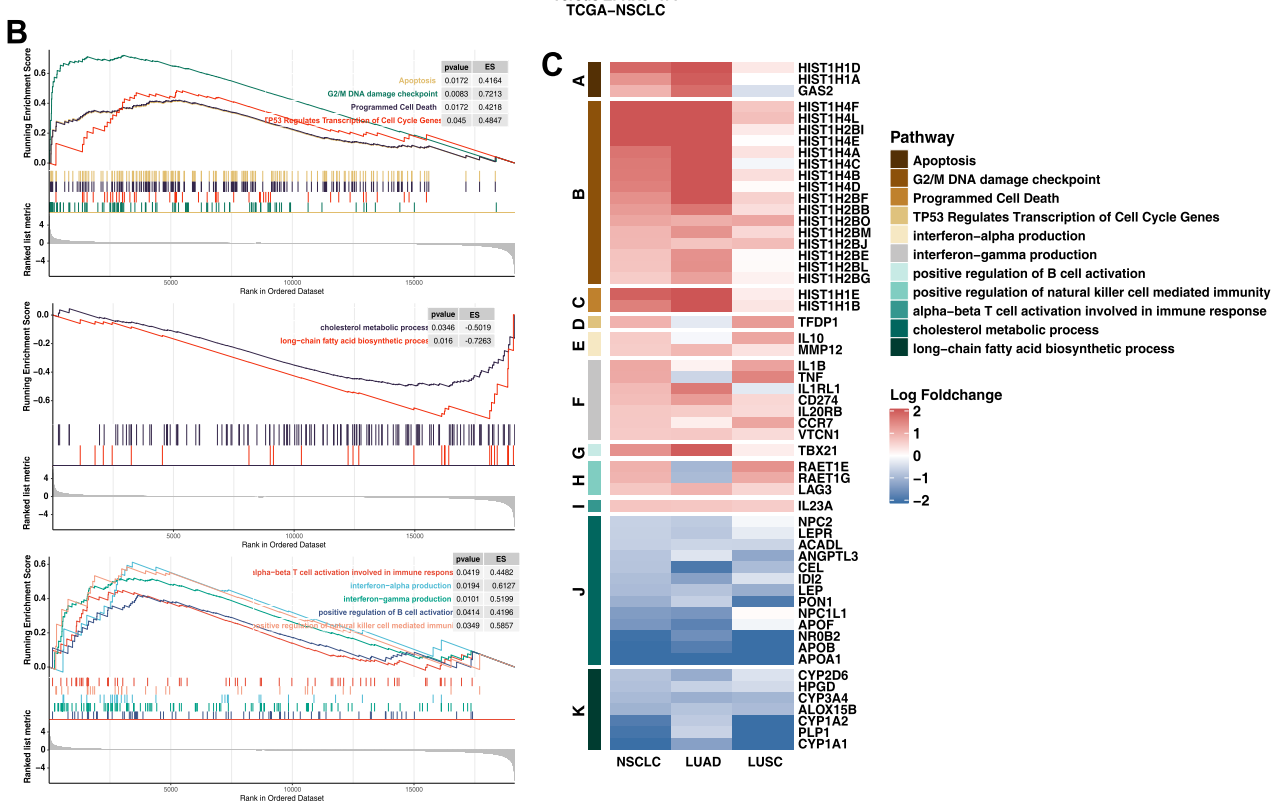
B
Running Enrichment Score
Ranked list metric
Rank in Ordered Dataset
pvalue ES
Apoptosis 0.0172 0.4164
G2/M DNA damage checkpoint 0.0083 0.7213
Programmed Cell Death 0.0172 0.4218
TP53 Regulates Transcription of Cell Cycle Genes 0.045 0.4847
cholesterol metabolic process 0.0346 −0.5019
long−chain fatty acid biosynthetic process 0.016 −0.7263
alpha−beta T cell activation involved in immune response 0.0419 0.4482
interferon−alpha production 0.0194 0.6127
interferon−gamma production 0.0101 0.5199
positive regulation of B cell activation 0.0414 0.4196
positive regulation of natural killer cell mediated immun 0.0349 0.5857
C
A
B
C
D
E
F
G
H
I
J
K
HIST1H1D
HIST1H1A
GAS2
HIST1H4F
HIST1H4L
HIST1H2BI
HIST1H4E
HIST1H4A
HIST1H4C
HIST1H4B
HIST1H4D
HIST1H2BF
HIST1H2BB
HIST1H2BO
HIST1H2BM
HIST1H2BJ
HIST1H2BE
HIST1H2BL
HIST1H2BG
HIST1H1E
HIST1H1B
TFDP1
IL10
MMP12
IL1B
TNF
IL1RL1
CD274
IL20RB
CCR7
VTCN1
TBX21
RAET1E
RAET1G
LAG3
IL23A
NPC2
LEPR
ACADL
ANGPTL3
CEL
IDI2
LEP
PON1
NPC1L1
APOF
NR0B2
APOB
APOA1
CYP2D6
HPGD
CYP3A4
ALOX15B
CYP1A2
PLP1
CYP1A1
NSCLC LUAD LUSC
Pathway
Apoptosis
G2/M DNA damage checkpoint
Programmed Cell Death
TP53 Regulates Transcription of Cell Cycle Genes
interferon−alpha production
interferon−gamma production
positive regulation of B cell activation
positive regulation of natural killer cell mediated immunity
alpha−beta T cell activation involved in immune response
cholesterol metabolic process
long−chain fatty acid biosynthetic process
Log Foldchange
2
1
0
−1
−2

◂**Fig. 5** Transcriptome biological function traits of ZFHX3-MT and ZFHX3-WT tumors in the TCGA-NSCLC cohort. **a** Differences in pathway activities scored by GSEA between ZFHX3-MT and ZFHX3-WT tumors in the TCGA-NSCLC cohort. Enrichment results with significant associations between ZFHX3-MT and ZFHX3-WT tumors are shown. The blue bar indicates that the enrichment score (ES) of the pathway is more than 0, while the green bar indicates that the ES of the pathway is less than 0. **b** GSEA of hallmark gene sets downloaded from MSigDB. All transcripts were ranked by the log2 (fold change) between ZFHX3-MT and ZFHX3-WT tumors in the TCGA-NSCLC cohort. Each run was performed with 1000 permutations. Enrichment results with significant associations between ZFHX3-MT and ZFHX3-WT tumors are shown. **c** Heatmap depicting the mean differences in the enrichment results with significant associations between ZFHX3-MT and ZFHX3-WT tumors in the TCGA-NSCLC, LUAD, and LUSC cohorts. The *x*-axis of the heatmap indicates different histological subtypes, and the y-axis indicates gene names and pathway signatures between ZFHX3-MT and ZFHX3-WT tumors in TCGA-NSCLC, LUAD, and LUSC. Red indicates upregulation, while blue indicates downregulation

ICI treatment in NSCLC. ZFHX3-MT was strongly associated with better OS, increased tumor immunogenicity, antitumor immune response ability, and the number of DDR pathway mutations. In addition, in the GDSC database, there was no significant difference in the sensitivity of common chemotherapy drugs between ZFHX3-MT and ZFHX3-WT NSCLC, LUAD, and LUSC cell lines (Supplementary Fig. S4), which suggests that ZFHX3-MT may have no significant predictive significance for chemotherapy in patients with lung cancer.

Zinc finger homeobox 3 (ZFHX3) was initially identified as ATBF1, a transcription factor that encoded four homeobox domains and 23 zinc fingers; ZFHX3 was shown to be involved in suppressing alpha-fetoprotein transcription [34, 35]. It was identified as a candidate tumor suppressor gene for prostate, breast, and gastric cancers, which acted by inducing cell cycle arrest [36–38]. ZFHX3 is frequently mutated in metastatic or high-grade human cancers, and many of the mutations are frameshifting and thus function inactivating [34, 35, 39]. Although these studies indicate an important role of ZFHX3 in cancers, it is unknown what ZFHX3 mutations exert function in NSCLC patients receiving ICI treatment. Furthermore, we have summarized the possible mechanisms underlying the improved efficacy and prognosis in ZFHX3-MT NSCLC receiving ICIs (Fig. 7).

The immunogenicity of the tumor is the basis for the initiation of the antitumor immune response, and higher frequency somatic mutations may cause tumor cells to produce more new antigens to enhance the immune killing abilities of T cells to tumor cells [40]. In addition, the immunogenicity of the tumor is also affected by factors in the TME, such as the efficiency of antigen processing and presentation of DCs, the most powerful antigen-presenting cells in the body [41]. The TME is closely related to the efficacy of ICIs in patients with lung cancer. For example, CD4 + T cells are associated with a better efficacy of immunotherapy [42]. Therefore, higher TMB, NAL, DCs, and CD4 + T cells may be why ICIs are more effective in ZFHX3-MT patients than in ZFHX3-WT patients.

In recent years, studies have shown that GEPs can be used as a novel potential predictor of the efficacy of immunotherapy [43, 44]. Jiang et al. [44] showed that a T-cell inflamed GEP is related to the clinical benefit of patients receiving ICI treatment. In addition, they evaluated CD8A, CD8B, GZMA, GZMB, and PRF1 expression levels to evaluate tumor cytotoxic T lymphocyte (CTL) infiltration levels, and found that the survival time of immunotherapy patients was significantly prolonged in the high-infiltration CTL groups. In addition, CD8 + T cells can be recruited to enhance immune infiltration and antitumor immunity by chemokines such as CXCL9 and CXCL10 [45]. Therefore, chemokines (such as CXCL10 and CCL5) and molecules related to cytolytic activity (such as GZMA) that are highly expressed at the mRNA level may be one of the reasons why the efficacy of ICIs is better in ZFHX3-MT patients than in ZFHX3-WT patients.

The DDR pathway is critical for maintaining genomic integrity. Alterations in the DDR pathway increase genomic instability and are associated with higher TMB. The previous studies have shown that mutations in the DDR pathway may serve as a potential predictive biomarker for ICI treatment and improve the clinical results of ICI treatment [15, 16]. Therefore, more DDR pathway mutations may be one of the reasons why ICIs are more effective in ZFHX3-MT patients than in ZFHX3-WT patients.

Studies have shown that IFN-γ can reduce the infiltration of Tregs, thereby enhancing the antitumor immune effect [46]. In addition, the expression profile of IFN-γ-related GEP can predict the clinical outcome of PD-1 treatment [43]. Studies have shown that cholesterol can be combined with the TCRβ transmembrane region or that disrupting the TCR signaling pathway further inhibits the antitumor activity of T cells [47, 48]. Cholesterol affects immune cells and promotes the metastasis and recurrence of breast cancer [49]. Ma et al. found that high cholesterol will promote the expression of T-cell immune checkpoints, making T cells more easily inhibited, thus losing antitumor function [50]. GSEA showed that immune response-related pathways (including interferon-gamma production, alpha–beta T-cell activation involved in the immune response, etc.) are significantly upregulated in ZFHX3-MT patients. In contrast, the cholesterol metabolic process was significantly downregulated in patients with ZFHX3-MT. Further comparison of core gene expression in these pathways revealed that the expression of core genes in the interferon-gamma production-related pathway in ZFHX3-MT patients was significantly upregulated, and core gene expression of the cholesterol metabolic process was significantly downregulated.

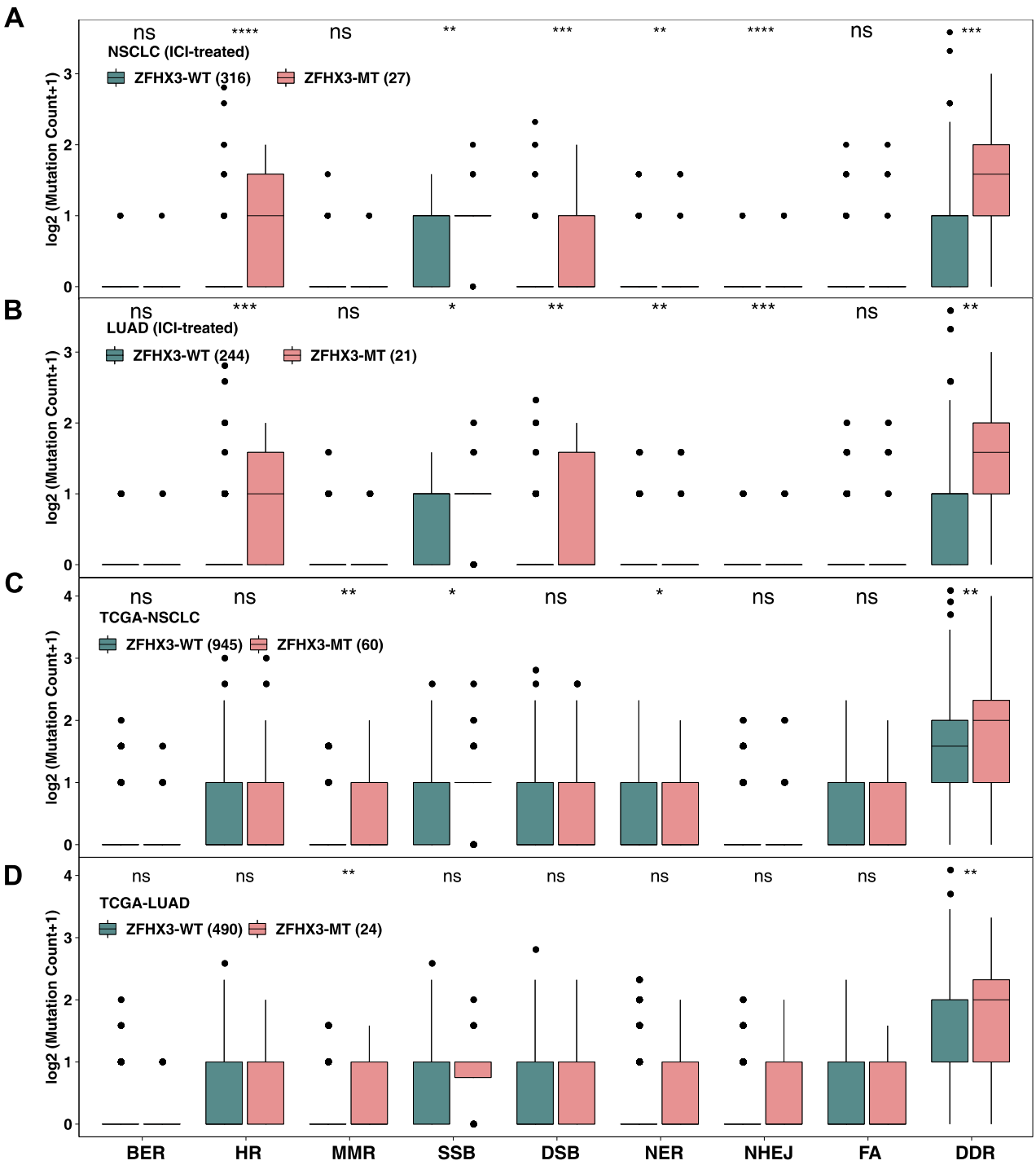

Fig. 6 Comparison of DNA damage-related gene set alterations between ZFHX3-MT and ZFHX3-WT tumors in cell lines from the ICI-treated NSCLC (**a**), ICI-treated LUAD (**b**), TCGA-NSCLC (**c**), and TCGA-LUAD (**d**) cohorts. (*, $P<0.05$; **, $P<0.01$; ***, $P<0.001$, ****, $P<0.0001$, Mann–Whitney U test)

Therefore, the GSEA results and gene expression profile also provide evidence that ZFHX3-MT patients can benefit more from ICI treatment than ZFHX3-WT patients.

We found that, in LUSC, there was no significant difference between ZFHX3-MT and ZFHX3-WT tumors in immune cell infiltration patterns, immune-related gene profiles, and number of mutations in the DDR pathway. Lambrechts et al. suggest that there are differences between stromal cell marker genes and tumor stromal cell subtypes in LUAD and LUSC tumors; moreover, the low expression

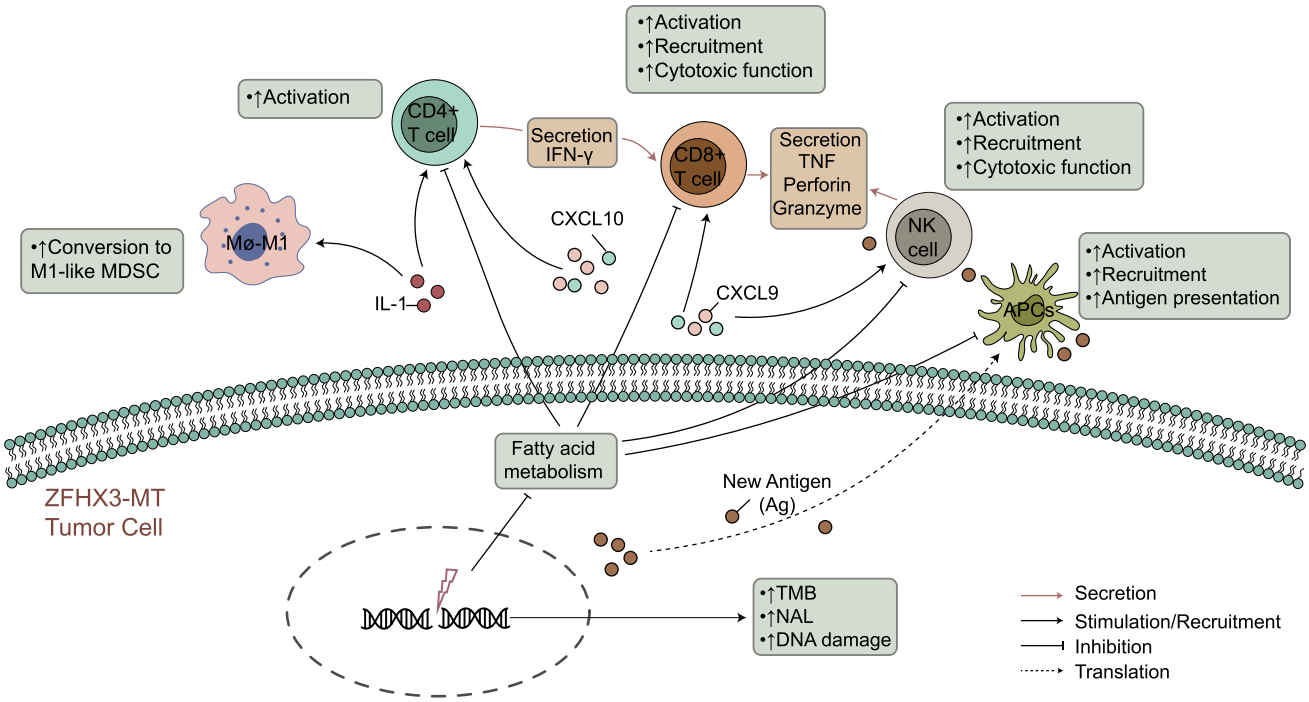

Fig. 7 The possible mechanism underlying the improved efficacy and prognosis in ZFHX3-MT NSCLC receiving ICIs

of CD8 + T-cell cluster genes in LUSC is associated with worse survival prognosis. Therefore, these findings suggest that the presence of the TME between LUAD and LUSC is different [51].

This study explored the association between the prognosis of NSCLC immunotherapy and specific mutated genes and tried to clarify the possible mechanism of ZFHX3-MT as an independent predictive marker of the prognosis of NSCLC immunotherapy. However, there are still some limitations. First, this study included only one NSCLC immunotherapy cohort, and there was bias in screening biomarkers for the prognosis of NSCLC immunotherapy. Second, the immunotherapy cohort used targeted sequencing (the Memorial Sloan Kettering-Integrated Mutation Profiling of Actionable Cancer Targets [MSK-IMPACT] panel) to detect gene mutations. Finally, our analysis discussed only the two most important subtypes of NSCLC; the remaining subtypes were not discussed. Therefore, more research involving a large number of samples and diverse ethnic groups is needed for analysis and validation.

Conclusions

The study found that ZFHX3 mutations are independent predictors of the prognosis of NSCLC immunotherapy. ZFHX3-MT is associated with longer OS after immunotherapy, and ZFHX3-MT is positively correlated with known predictive markers of immunotherapy, including TMB, NAL, immune-related genes, immune cells, and the number of DDR pathway mutations. Therefore, ZFHX3 mutations can be used as a novel potential predictive marker to guide NSCLC ICI treatment. A series of prospective clinical studies and molecular mechanism explorations are still needed in the future.

Acknowledgements We would like to thank the biotrainee, Dr. Jianming Zeng (University of Macau), XiaoYa HuaTu, Lianchuan Biotechnology Limited (subsidiary of LC Sciences, Hangzhou, China), and Haplox Biotechnology Co., Ltd.

Author contributions Conceptualization, LLG, WLZ, and JZ; formal analysis, JXZ, NNZ, AQL, PL, and XC; software, JXZ, NNZ, AQL, and PL; supervision, LLG, WLZ, and JZ; visualization, JXZ, NNZ, AQL, and PL; writing–original draft, JXZ, NNZ, AQL, PL, XC, HJD, and SJK; writing–review & editing, JXZ, NNZ, AQL, PL, and XC.

Funding This work was supported by grants from the National Natural Science Foundation of China (Nos. 81572244, 81602631, 81672267, 81772458, 81871859, and 81972809); Natural Science Foundation of Guangdong Province (key) (2015A030311028); The Clinical Research Initiative Project of Southern Medical University (LC2016ZD029 and LC2019ZD016); Major Basic Research Projects and Major Applied Research Projects of Educational Commission of Guangdong Province (2017KZDXM015).

Availability of data and material All of the data we used in this study were publicly available as described in the Method section.

Compliance with ethical standards

Conflict of interests The authors declare that they have no conflict interests.

References

1. Fitzmaurice C, Allen C, Barber RM et al (2017) Global, regional, and national cancer incidence, mortality, years of life lost, years lived with disability, and disability-adjusted life-years for 32 cancer groups, 1990 to 2015. JAMA Oncol 3:524. https://doi.org/10.1001/jamaoncol.2016.5688
2. Garon EB, Rizvi NA, Hui R et al (2015) Pembrolizumab for the treatment of non–small-cell lung cancer. N Engl J Med 372:2018–2028. https://doi.org/10.1056/NEJMoa1501824
3. Havel JJ, Chowell D, Chan TA (2019) The evolving landscape of biomarkers for checkpoint inhibitor immunotherapy. Nat Rev Cancer 19:133–150
4. Zou W, Wolchok JD, Chen L (2016) PD-L1 (B7–H1) and PD-1 pathway blockade for cancer therapy: Mechanisms, response biomarkers, and combinations. Sci Transl Med. https://doi.org/10.1126/scitranslmed.aad7118
5. Wang S, He Z, Wang X et al (2019) Antigen presentation and tumor immunogenicity in cancer immunotherapy response prediction. Elife. https://doi.org/10.7554/eLife.49020
6. Boeri M, Milione M, Proto C et al (2019) Circulating miRNAs and PD-L1 tumor expression are associated with survival in advanced NSCLC patients treated with immunotherapy: A prospective study. Clin Cancer Res 25:2166–2173
7. Cristescu R, Mogg R, Ayers M et al (2018) Pan-tumor genomic biomarkers for PD-1 checkpoint blockade-based immunotherapy. Science. https://doi.org/10.1126/science.aar3593
8. Riaz N, Havel JJ, Kendall SM et al (2016) Recurrent SERPINB3 and SERPINB4 mutations in patients who respond to anti-CTLA4 immunotherapy. Nat Genet 48:1327–1329. https://doi.org/10.1038/ng.3677
9. Wang F, Zhao Q, Wang YN et al (2019) Evaluation of POLE and POLD1 mutations as biomarkers for immunotherapy outcomes across multiple cancer types. JAMA Oncol 5:1504–1506
10. Wu HX, Chen YX, Wang ZX et al (2019) Alteration in TET1 as potential biomarker for immune checkpoint blockade in multiple cancers. J Immunother Cancer 7:264. https://doi.org/10.1186/s40425-019-0737-3
11. Dong Z-Y, Zhong W-Z, Zhang X-C et al (2017) Potential predictive value of TP53 and KRAS mutation status for response to PD-1 blockade immunotherapy in lung adenocarcinoma. Clin Cancer Res 23:3012–3024. https://doi.org/10.1158/1078-0432.CCR-16-2554
12. Ji M, Liu Y, Li Q et al (2016) PD-1/PD-L1 expression in non-small-cell lung cancer and its correlation with EGFR/KRAS mutations. Cancer Biol Ther 17:407–413. https://doi.org/10.1080/15384047.2016.1156256
13. Spigel DR, Schrock AB, Fabrizio D et al (2016) Total mutation burden (TMB) in lung cancer (LC) and relationship with response to PD-1/PD-L1 targeted therapies. J Clin Oncol 34:9017–9017. https://doi.org/10.1200/jco.2016.34.15_suppl.9017
14. Lin A, Wei T, Meng H et al (2019) Role of the dynamic tumor microenvironment in controversies regarding immune checkpoint inhibitors for the treatment of non-small cell lung cancer (NSCLC) with EGFR mutations. Mol Cancer 18:139
15. Wang J, Wang Z, Zhao J et al (2018) Co-mutations in DNA damage response pathways serve as potential biomarkers for immune checkpoint blockade. Cancer Res. https://doi.org/10.1158/0008-5472.CAN-18-1814
16. Teo MY, Seier K, Ostrovnaya I et al (2018) Alterations in DNA damage response and repair genes as potential marker of clinical benefit from PD-1/PD-L1 blockade in advanced urothelial cancers. J Clin Oncol 36:1685–1694. https://doi.org/10.1200/JCO.2017.75.7740
17. Samstein RM, Lee C-H, Shoushtari AN et al (2019) Tumor mutational load predicts survival after immunotherapy across multiple cancer types. Nat Genet 51:202–206. https://doi.org/10.1038/s41588-018-0312-8
18. Colaprico A, Silva TC, Olsen C et al (2016) TCGAbiolinks: an R/Bioconductor package for integrative analysis of TCGA data. Nucleic Acids Res 44:e71–e71. https://doi.org/10.1093/nar/gkv1507
19. Cerami E, Gao J, Dogrusoz U et al (2012) The cBio Cancer Genomics Portal: An open platform for exploring multidimensional cancer genomics data. Cancer Discov 2:401–404. https://doi.org/10.1158/2159-8290.CD-12-0095
20. Hellmann MD, Nathanson T, Rizvi H et al (2018) Genomic features of response to combination immunotherapy in patients with advanced non-small-cell lung cancer. Cancer Cell 33:843–852.e4. https://doi.org/10.1016/j.ccell.2018.03.018
21. Newman AM, Liu CL, Green MR et al (2015) Robust enumeration of cell subsets from tissue expression profiles. Nat Methods 12:453–457. https://doi.org/10.1038/nmeth.3337
22. Thorsson V, Gibbs DL, Brown SD et al (2018) The immune landscape of cancer. Immunity 48:812–830.e14. https://doi.org/10.1016/j.immuni.2018.03.023
23. Chalmers ZR, Connelly CF, Fabrizio D et al (2017) Analysis of 100,000 human cancer genomes reveals the landscape of tumor mutational burden. Genome Med 9:34. https://doi.org/10.1186/s13073-017-0424-2
24. Yu G, Wang L-G, Han Y, He Q-Y (2012) clusterProfiler: an R package for comparing biological themes among gene clusters. Omi A J Integr Biol 16:284–287. https://doi.org/10.1089/omi.2011.0118
25. Subramanian A, Tamayo P, Mootha VK et al (2005) Gene set enrichment analysis: A knowledge-based approach for interpreting genome-wide expression profiles. Proc Natl Acad Sci 102:15545–15550. https://doi.org/10.1073/pnas.0506580102
26. Gu Z, Eils R, Schlesner M (2016) Complex heatmaps reveal patterns and correlations in multidimensional genomic data. Bioinformatics 32:2847–2849. https://doi.org/10.1093/bioinformatics/btw313
27. Luo P, Lin A, Li K et al (2019) DDR pathway alteration, tumor mutation burden, and cisplatin sensitivity in small cell lung cancer: difference detected by whole exome and targeted gene sequencing. J Thorac Oncol 14:e276–e279
28. Le DT, Uram JN, Wang H et al (2015) PD-1 blockade in tumors with mismatch-repair deficiency. N Engl J Med 372:2509–2520. https://doi.org/10.1056/NEJMoa1500596
29. Rizvi NA, Hellmann MD, Snyder A et al (2015) Mutational landscape determines sensitivity to PD-1 blockade in non–small cell lung cancer. Science. https://doi.org/10.1126/science.aaa1348
30. Gao J, Shi LZ, Zhao H et al (2016) Loss of IFN-γ pathway genes in tumor cells as a mechanism of resistance to anti-CTLA-4 therapy. Cell 167:397–404.e9. https://doi.org/10.1016/j.cell.2016.08.069
31. Zaretsky JM, Garcia-Diaz A, Shin DS et al (2016) Mutations associated with acquired resistance to PD-1 blockade in melanoma. N Engl J Med 375:819–829. https://doi.org/10.1056/NEJMoa1604958
32. Gainor JF, Shaw AT, Sequist LV et al (2016) EGFR mutations and ALK rearrangements are associated with low response rates to PD-1 pathway blockade in non-small cell lung cancer: A

retrospective analysis. Clin Cancer Res 22:4585–4593. https://doi.org/10.1158/1078-0432.CCR-15-3101
33. Peng W, Chen JQ, Liu C et al (2016) Loss of PTEN promotes resistance to T cell-mediated immunotherapy. Cancer Discov 6:202–216. https://doi.org/10.1158/2159-8290.CD-15-0283
34. Hu Q, Zhang B, Chen R et al (2019) ZFHX3 is indispensable for ERβ to inhibit cell proliferation via MYC downregulation in prostate cancer cells. Oncogenesis 8:28. https://doi.org/10.1038/s41389-019-0138-y
35. Fu C, An N, Liu J et al (2020) The transcription factor ZFHX3 is crucial for the angiogenic function of hypoxia-inducible factor 1α in liver cancer cells. J Biol Chem 295:7060–7074. https://doi.org/10.1074/jbc.RA119.012131
36. Jung C-G, Kim H-J, Kawaguchi M et al (2005) Homeotic factor ATBF1 induces the cell cycle arrest associated with neuronal differentiation. Development 132:5137–5145. https://doi.org/10.1242/dev.02098
37. Kataoka H, Miura Y, Joh T et al (2001) Alpha-fetoprotein producing gastric cancer lacks transcription factor ATBF1. Oncogene 20:869–873. https://doi.org/10.1038/sj.onc.1204160
38. Zaw KTT, Sato N, Ikeda S et al (2017) Association of ZFHX3 gene variation with atrial fibrillation, cerebral infarction, and lung thromboembolism: An autopsy study. J Cardiol 70:180–184. https://doi.org/10.1016/j.jjcc.2016.11.005
39. Grasso CS, Wu Y-M, Robinson DR et al (2012) The mutational landscape of lethal castration-resistant prostate cancer. Nature 487:239–243. https://doi.org/10.1038/nature11125
40. Gubin MM, Artyomov MN, Mardis ER, Schreiber RD (2015) Tumor neoantigens: building a framework for personalized cancer immunotherapy. J Clin Invest 125:3413–3421. https://doi.org/10.1172/JCI80008
41. Mellman I, Steinman RM (2001) Dendritic Cells. Cell 106:255–258. https://doi.org/10.1016/S0092-8674(01)00449-4
42. Spitzer MH, Carmi Y, Reticker-Flynn NE et al (2017) Systemic immunity is required for effective cancer immunotherapy. Cell 168:487–502.e15. https://doi.org/10.1016/j.cell.2016.12.022
43. Ayers M, Lunceford J, Nebozhyn M et al (2017) IFN-γ–related mRNA profile predicts clinical response to PD-1 blockade. J Clin Invest 127:2930–2940. https://doi.org/10.1172/JCI91190
44. Jiang P, Gu S, Pan D et al (2018) Signatures of T cell dysfunction and exclusion predict cancer immunotherapy response. Nat Med 24:1550–1558. https://doi.org/10.1038/s41591-018-0136-1
45. Peng D, Kryczek I, Nagarsheth N et al (2015) Epigenetic silencing of TH1-type chemokines shapes tumour immunity and immunotherapy. Nature 527:249–253. https://doi.org/10.1038/nature15520
46. Overacre-Delgoffe AE, Chikina M, Dadey RE et al (2017) Interferon-γ drives treg fragility to promote anti-tumor immunity. Cell 169:1130–1141.e11. https://doi.org/10.1016/j.cell.2017.05.005
47. Swamy M, Beck-Garcia K, Beck-Garcia E et al (2016) A cholesterol-based allostery model of t cell receptor phosphorylation. Immunity 44:1091–1101. https://doi.org/10.1016/j.immuni.2016.04.011
48. Wang F, Beck-García K, Zorzin C et al (2016) Inhibition of T cell receptor signaling by cholesterol sulfate, a naturally occurring derivative of membrane cholesterol. Nat Immunol 17:844–850. https://doi.org/10.1038/ni.3462
49. Baek AE, Yu YRA, He S et al (2017) The cholesterol metabolite 27 hydroxycholesterol facilitates breast cancer metastasis through its actions on immune cells. Nat Commun 8:864. https://doi.org/10.1038/s41467-017-00910-z
50. Ma X, Bi E, Lu Y et al (2019) Cholesterol induces CD8+ T cell exhaustion in the tumor microenvironment. Cell Metab 30:143–156.e5. https://doi.org/10.1016/j.cmet.2019.04.002
51. Lambrechts D, Wauters E, Boeckx B et al (2018) Phenotype molding of stromal cells in the lung tumor microenvironment. Nat Med 24:1277–1289. https://doi.org/10.1038/s41591-018-0096-5